FULL PAPER

Multilayered Blood Capillary Analogs in Biodegradable Hydrogels for In Vitro Drug Permeability Assays

*Hiroaki Yoshida, Michiya Matsusaki, and Mitsuru Akashi**

Blood capillaries are crucial for the biological evaluation of drug diffusion to target tissues, and the penetration of cancer cells or viruses. Since most capillaries have a bilayered structure consisting of a monolayer of endothelial cells (ECs) and surrounding smooth muscle cells (SMCs), the in vitro reconstruction of this bilayered structure is a key challenge for pharmaceutical and biomedical applications. Here, a unique technology to construct size, length, orientation, and layer-number controllable blood capillary networks in biodegradable hydrogels is reported. Uniaxial microchannels are prepared inside biodegradable hydrogels by the simple extraction of silica capillary tubes. The channel size, length, and distance of the uniaxial channels are easily controlled by altering these parameters of the silica tubes. The inner surfaces of the channels are successfully covered by bilayered structures consisting of ECs and SMCs by a hierarchical cell manipulation technique. Notably, serum albumin, which has an approximately 8 nm size, cannot penetrate this capillary wall during several hours of incubation due to the high blood vessel wall barrier property. This suggests a successful reconstruction of multilayered blood capillary networks possessing similar barrier function as native blood capillaries. Moreover, these capillary networks can be completely collected by the selective degradation of the surrounding hydrogels. This technique will be an innovative and versatile approach for in vitro permeability assays of drugs, drug delivery carriers, and cancer cells.

1. Introduction

A blood vessel is generally composed of three distinct layers: a single layer of endothelial cells (ECs) as the inner surface (the intima), smooth muscle cell (SMC) layers (the media), and a fibroblast cell outer-layer (the adventitia).[1,2] The layer number of SMCs varies depending on the size of the vessel and its anatomical location. For example, a blood capillary is composed of a bilayered structure of ECs and SMCs (or pericytes). Blood capillaries are present in almost all tissues and organs, and play a pivotal role in circulating nutrients, oxygen, and blood cells, as well as in drug penetration, the metastasis of cancer cells, and in vivo imaging.[3–5] In general, the functions of blood capillaries are evaluated from in vivo animal experiments, but their detailed biological and biochemical functions in response to chemical and physical stimuli cannot be understood well due to both the analytical difficulty in experimental data and the differences between human and animal.[6,7] Thus, the in vitro reconstruction of a blood capillary with a controlled morphology, layer number, and permeability is a challenge in the biomaterial field in order to develop a novel assay system for the in vitro evaluation of vascular properties. For example, the enhanced permeability and retention (EPR) effect of tumor blood capillaries is well known for the tumor targeting of drug delivery systems (DDS) using a nanocarrier of less than 100 nm in diameter.[8] However, Kano et al. recently reported that the blood capillaries in a solid tumor show an insufficient EPR effect, probably due to the supporting properties of the surrounding SMCs or pericytes on EC barrier function.[9] Thus, the layer number and components of a blood capillary are crucial for drug permeability in pharmaceutical and biomedical applications. Accordingly, if an in vitro drug permeability assay system can be developed using blood capillary models possessing a controlled layer structure, then it will be a powerful tool for DDS and pharmaceutical applications. Moreover, drug penetration, the metastasis of cancer cells, and pathogen invasion assay systems based on these reconstructed blood capillaries will represent innovative technologies.

EC monolayers cultured on a porous membrane (transwell) have been studied as an in vitro vascular model for the investigation of EC barrier functions by using the diffusion of fluorescent dyes, and by evaluating the transendothelial electrical resistance (TER).[7,10] However, due to the lack of layered structures, the properties of a naked blood capillary could not be simulated. Furthermore, the nonspecific adsorption of dye molecules onto the transwell affects the evaluation of EC barrier functions, and thus this transwell system cannot be used for flow-cultures to approximate blood flow conditions. Therefore,

H. Yoshida, Dr. M. Matsusaki, Prof. M. Akashi
Department of Applied Chemistry
Graduate School of Engineering
Osaka University
2-1 Yamada-oka, Suita, Osaka 565-0871, Japan
E-mail: akashi@chem.eng.osaka-u.ac.jp
Dr. M. Matsusaki
PRESTO, Japan Science and Technology Agency (JST)
4-1-8 Honcho Kawaguchi, Saitama, Japan

DOI: 10.1002/adfm.201201905

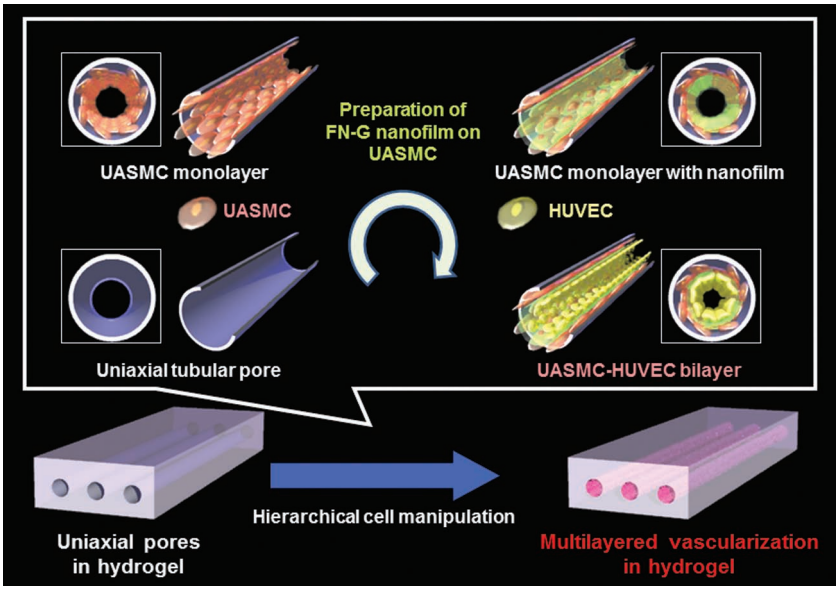

Figure 1. Schematic illustration of the in vitro reconstruction of multilayered blood capillary analogs in biodegradable hydrogels by the hierarchical cell manipulation technique.

a novel technology to fabricate an in vitro blood capillary assay system to simulate native layered structures, a tubular morphology, and flow culture conditions is desirable.

Here, we propose for the first time a simple and versatile method to construct multilayered blood capillaries inside biodegradable hydrogels (**Figure 1**). Hydrogels are attractive soft materials used for biomedical applications due to their water-swelling structure and material properties similar to living tissues.[11,12] Moreover, hydrogels are a good candidate to control the permeability of proteins or polymers by altering the crosslinking mesh size, and to prevent nonspecific adsorption due to their hydrophilic properties. Recently, microfluidic channels covered with ECs inside poly(dimethylsiloxane) (PDMS) gels were reported as a model for blood capillaries.[13–15] However, the drug permeability from the EC surfaces cannot be analyzed by PDMS systems, because PDMS does not have good substance permeability, although it have high oxygen permeability. In this study, poly(γ-glutamic acid) (γ-PGA) was employed to fabricate disulfide-crosslinked hydrogels because of the ease in controlling the crosslinking networks, high-water content, biodegradability, and biocompatibility.[16,17] Uniaxial microchannels inside the γ-PGA gels were prepared by using silica capillary tubes. The disulfide-linkage (-S-S-) is rapidly cleaved to thiol groups (-SH HS-) using biocompatible reductants such as cysteine or glutathione (hydrogel template method),[18–20] and thus blood capillary networks can be safely and easily collected by the decomposition of the disulfide-crosslinked γ-PGA (γ-PGA-SS) gels with reductants. These obtained blood capillary networks could be useful as implantable artificial blood capillaries.

Recently, we developed a simple and unique technology, the hierarchical cell manipulation method, to fabricate multilayered cellular constructs by preparing nanometer-sized extracellular matrix (ECM) films on the surface of each cell layer.[21,22] This technique can allow the preparation of the desired multilayered structures on varied surfaces, even through the inner wall of tubular channels, because the driving force is the adsorption of the cells and nanofilm components. In this study, we applied this method to the inner channels of γ-PGA-SS gels to construct multilayered blood capillary structures using human umbilical vein endothelial cells (HUVECs) and human umbilical artery smooth muscle cells (UASMCs). To elucidate the blood barrier effect of these constructed capillaries, the time-dependent permeation of bovine serum albumin (BSA) of ca. 8 nm size was analyzed in detail. This simple and versatile approach would be useful for the in vitro assay of drug permeability through multilayered blood capillaries in the pharmaceutical and biomedical fields.

2. Results and Discussion

2.1. Preparation of Uniaxial Tubular Microchannels in Hydrogels

Uniaxial tubular porous structures in the γ-PGA-SS gels were prepared by the hybrid gel formation of γ-PGA and silica capillary tubes of 620 μm diameter, and the subsequent extraction of these silica tubes (**Figure 2**a). A γ-PGA polymer solution was mixed with the disulfide crosslinker cystamine, the GRGDS peptide, and water soluble carbodiimide (Scheme S1, Supporting Information). The chemical structures of the obtained γ-PGA-SS gels were characterized by UV-vis spectroscopy using Ellman's method and by Fourier transform infrared spectroscopy (FTIR) analyses, as was done in our previous papers (data not shown).[18,19] The RGD peptide was employed to improve the cell adhesive properties of the γ-PGA gels.[23] The resultant solution was poured between 2 glass plates with a 2-mm silicon spacer and aligned silica tubes, and then incubated for 3 h at room temperature. After gelation, the silica tubes were gently extracted, and the obtained gels were washed with ultrapure water for 2 days. The diameter of the obtained microchannels was approximately 720 μm, which was slightly larger than the silica tube diameter due to swelling of the hydrogels (Figure 2b). The channel size was easily controllable depending on the diameter of the silica tubes inserted (Figure 2c and Figure S1). Furthermore, interconnected orthogonal-tubular channels were also successfully fabricated in the hydrogels by an orthogonal alignment of the silica capillaries (Figure S2, Supporting Information). Figure 2d shows time-lapse images of the rapid penetration of a methylene blue solution into the tubular channels with 720 μm size within 10 s, suggesting complete interconnectivity and usability as a flow culture devise (Video S1, Supporting Information). Since flow speed in channel Q (m^3/s) depends on the cross sectional area S (m^2), larger channel size should show higher penetration speed. Accordingly, we can control penetration rate depending on the pore diameter.

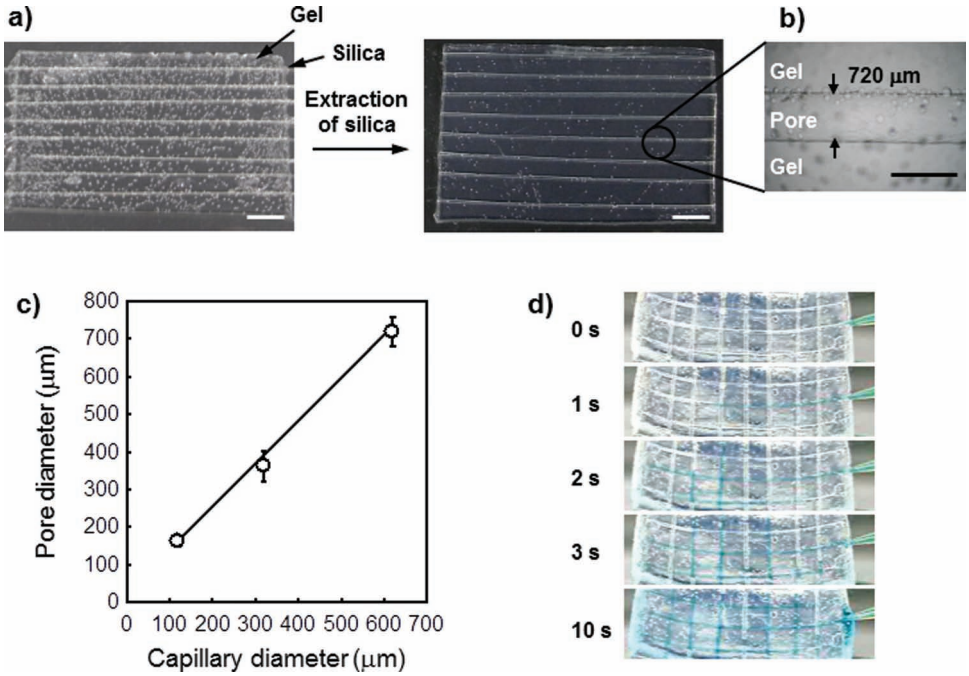

Figure 2. Preparation of γ-PGA-SS hydrogels with uniaxial tubular microchannels. a) The hybrid gel formation of γ-PGA and silica capillary tubes of 620 μm diameter (left) and the subsequent extraction of these silica tubes (right). The obtained gel size was about 4.5 cm × 7 cm. b) Phase contrast microscopic (Ph) image of the gels. c) Relationship between the diameter of the silica capillaries and the diameter of the obtained channels (n = 3). d) Time-lapse images of the rapid penetration of methylene blue solution into the orthogonal-tubular channels with 720 μm size of the γ-PGA-SS hydrogels constructed by an orthogonal alignment of the silica capillaries. See also Figure S2 and Video S1 in the Supporting Information. The white- and black-colored scale bars represent 1 cm and 1 mm, respectively.

2.2. Fabrication of Cellular Multilayers in Tubular Microchannels

The cellular multilayers were fabricated onto the surface of the inner wall of the tubular channels by the hierarchical cell manipulation technique.[21,22] Approximately 6-nm-thick fibronectin-gelatin (FN-G) layer-by-layer (LbL) films as a cell adhesive base layer were prepared on the surface of the tubular channels. LbL technique is an appropriate method to prepare nanometer- to micrometer-sized films on a substrate by alternate immersion into interactive polymer or protein solutions.[24,25] A HUVEC suspension was injected into the channels, and incubated by rotary culture for 48 h at 10 rpm. **Figure 3**a shows a macroscopic image from a confocal fluorescence microscope of the tubular channels covered with HUVECs fluorescently labeled

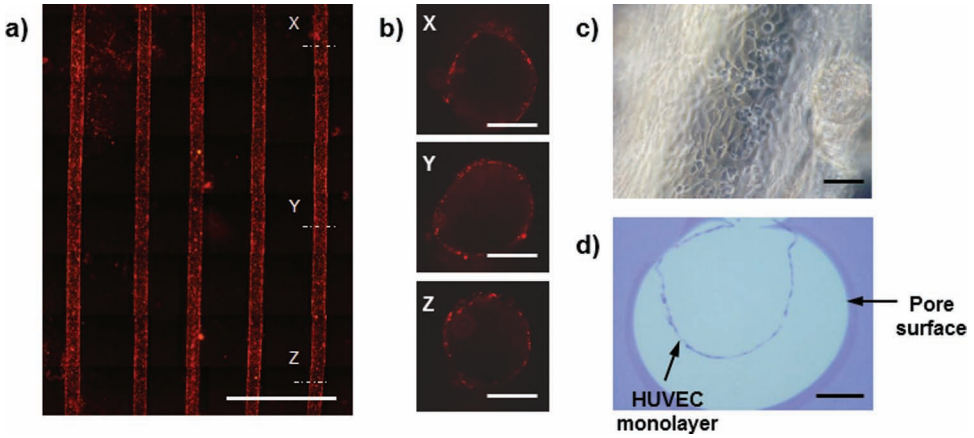

Figure 3. Formation of a HUVEC monolayer onto the microchannels of the γ-PGA-SS gels. Confocal fluorescent images of a) top and b) cross-sectional views of HUVECs fluorescently labeled with PKH26. c) Phase contrast images of HUVECs at the Y position in (a). The gel size was 2 cm × 1.5 cm. The cross-sectional images in (b) were observed at three different positions (X, Y, and Z) in (a). d) Hematoxylin-eosin (HE) stained images of the HUVEC monolayer at the Y position in (a). The scale bars are 5 mm in (a), 400 μm in (b), and 100 μm in (c) and (d).

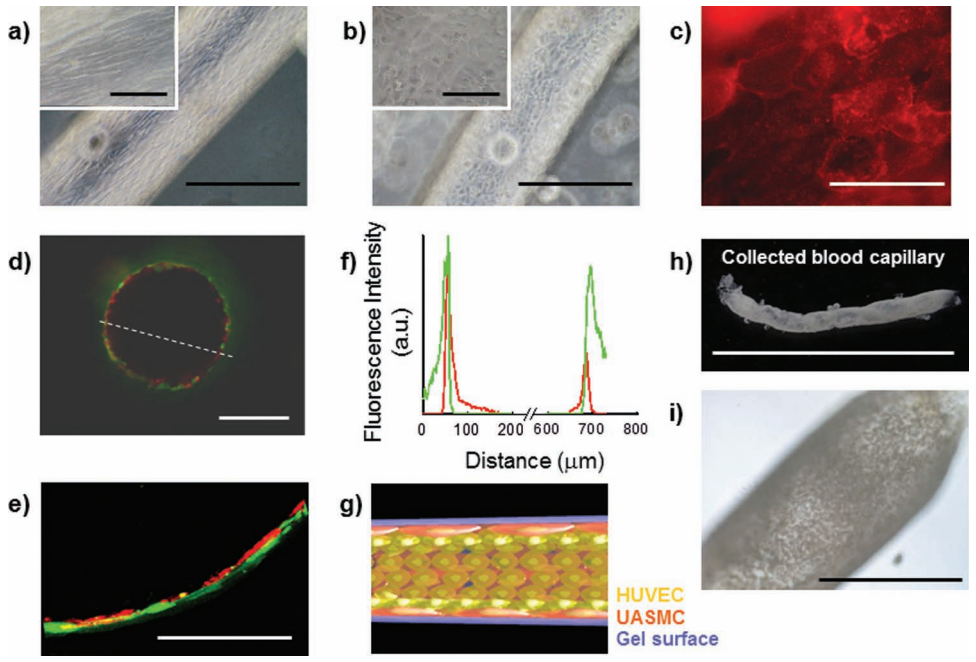

Figure 4. Fabrication of multilayered blood capillary analogs composed of UASMCs and HUVECs inside γ-PGA-SS gels. The phase contrast (Ph) images of a) are the UASMC monolayers prepared onto the surface of the inner gel walls and b) are HUVEC layers subsequently prepared on the UASMC layers. The insets show magnified images. c) An immunofluorescence image of the HUVEC layers on the UASMC monolayers immunostained with an anti-CD31 antibody. d) Confocal fluorescent microscopic images of the bilayer morphology of the cell tracker green-labeled UASMCs as the first layer and the PKH26-labeled HUVECs as the second layer. e) A magnified image of (d). f) Fluorescence intensity of the line-scanning along the dashed line in (d). g) Schematic illustration of a bilayer blood capillary formed in the gel. h) Photograph and i) Ph image of a blood capillary collected after the decomposition of the hydrogels by 12 h of incubation in culture medium with 10 mM L-cysteine. The scale bars are 600 μm in (a), (b), and (i), 150 μm in the insets of (a) and (b), 50 μm in (c), 400 μm in (d), 100 μm in (e), and 1 cm in (h).

with PKH26. The homogeneous adhesion of HUVECs over the entire surface of the channels was observed at the centimeter scale, and cross-sectional fluorescence images of the channels at different positions revealed a monolayered coverage by the HUVECs (Figure 3b). Furthermore, the phase contrast (Ph) image in Figure 3c reveals a spindle shape for the adhered HUVECs, and a histological cross-sectional image stained with hematoxylin-eosin (HE) also supported the homogeneous monolayered coverage of HUVECs inside the tubes (Figure 3d). The detachment of the HUVEC monolayer from the inner wall of the microchannels was due to technical reasons during the histological processing. This method is versatile enough to fabricate various kinds of cellular monolayers, such as human dermal fibroblast cells (FCs) and UASMCs, on the surface of the tubular channels (Figure S3 and S4, Supporting Information).

The bilayer structure consisting of HUVECs and UASMCs similar to a blood capillary in vivo was fabricated in the channels in the same manner. After preparation of the UASMC monolayers (**Figure 4**a), the FN-G nanofilms were fabricated on the surface of the UASMC layer to allow adhesion of the HUVECs as a second layer. The spindle morphology of the HUVECs was clearly observed after the preparation of the HUVEC second layer (Figure 4b). An immunofluorescence image of HUVECs immunostained with an anti-CD31 antibody clearly revealed junction formation of the HUVECs on the surface of the first layer of UASMCs (Figure 4c). To evaluate the bilayer structure of the HUVECs and UASMCs in detail, a fluorescence cross-sectional image was obtained by confocal microscopy. Figure 4d,e clearly shows the bilayer morphology of the cell tracker green-labeled UASMCs as the first layer, and the PKH26-labeled HUVECs as the second layer. The fluorescence intensity of the line-scanning in Figure 4d indicated a bilayered distribution of the HUVECs and UASMCs on the channel wall (Figure 4f). These results suggested that an artificial blood capillary construct was successfully fabricated in the channel surfaces of the hydrogels as shown in Figure 4g.

Since γ-PGA-SS gels are easily decomposed by the addition of biocompatible reductants such as cysteine,[18–20] we attempted to collect the artificial blood capillaries from the hydrogels. Figure 4h,i show the collected blood capillaries after the decomposition of the hydrogels by the addition of cysteine. Notably, capillaries of over 1 cm in length were easily obtained, and their diameters and lengths were completely maintained from the tubular channel structures in the hydrogels. Since we reported high cell viability in these constructs using our hydrogel template method,[18–20] these collected tubular tissues will be useful as an implantable artificial blood capillary.

2.3. Barrier Effect of the Blood Capillary Analog

One of the advantages of this method is its applications for permeability assays (blood barrier assay) due to the surrounding hydrogel networks, which allow the penetration of

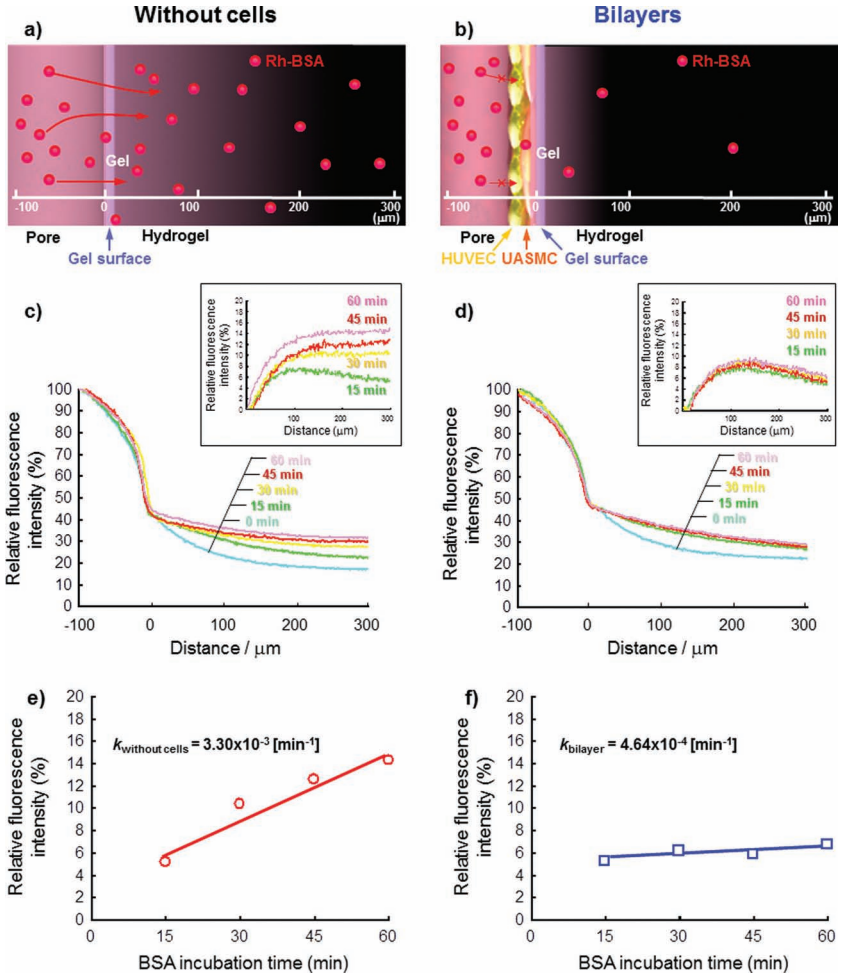

Figure 5. Barrier effect of the blood capillary analog. Schematic illustration of the BSA permeability of the hydrogels a) without or a) with the bilayers. c,d) Fluorescence intensity change in relation to the distance from the inner gel walls. The fluorescence intensity of the line-scanning shown in (a) and (b) was measured every 15 min, and normalized against the fluorescence intensity at the −100 μm position (at around the center of the channels). The intensity was an average value of over 10 replicates. The relative fluorescence intensity as compared to the initial intensity (0 min) was plotted in the insets of (c) and (d). e,f) The fluorescence intensity change at a distance of 300 μm and the diffusion rate constant *k*.

macromolecules. To elucidate the network size of the hydrogels, the penetration of fluorescein isothiocyanate-labeled dextran (FITC-Dex; M_w = 200 kDa) from the tubular channels into the gel networks was observed by confocal fluorescence microscopy. The fluorescent image after 24 h of incubation clearly showed the penetration of the FITC-Dex into the gel networks (Figure S5, Supporting Information), suggesting that the gel network size is at least over 50 nm, because the hydrodynamic diameter of FITC-Dex has been reported to be 50 nm.[9] Accordingly, major serum proteins such as albumin (M_w ≈ 65–70 kDa) and globulin (M_w ≈ 100–150 kDa) can be permeated from the tubular channels into the gel networks. If the bilayer structures of the HUVECs and UASMCs act as an artificial blood capillary, then these serum proteins should not penetrate into the gel networks. We analyzed the barrier effect of the bilayer structures using rhodamine-labeled bovine serum albumin (Rh-BSA) as compared to naked tubular channels. **Figure 5**a,b show schematic illustrations of the barrier effect assay, and a fluorescent image of the Rh-BSA in the channels at the initial stage is shown in Figure S6 (Supporting Information). The time-lapse fluorescence intensity of Rh-BSA diffusing from the channel interface to 300 μm inside the gels was measured over 60 min by line-scanning of the fluorescent images over this time period. In the case of the naked channels, the relative fluorescence intensity of the Rh-BSA increased with increasing incubation time, even at a 300-μm distance from the channel interface, suggesting that there was no barrier effect against the diffusion of the serum albumin (Figure 5c). On the other hand, the bilayer structures did not show any increase in the fluorescence intensity regardless of the incubation time, and the relative fluorescence intensity was decreased with increasing distance from the channel surface (Figure 5d). For the quantitative evaluation of BSA diffusion, the diffusion rate constant k at 300 μm from the channel surface was estimated from the inset in Figure 5c,d. The diffusion rate constant of the naked channels was 7.1-fold higher than that of the bilayer structures, and these results clearly supported a high barrier effect of the bilayer structures, much like a native blood capillary. The nonspecific adsorption of Rh-BSA onto the outermost HUVEC surfaces was not observed after washing the channels.

In this experiment, we stopped the penetration assays of BSA for 1 h. However, if the experiments were continued for a longer time, e.g., 1 day, higher penetration though transcellular pathway should be observed due to the endocytosis of albumin.[26–28] Actually, slight penetration (less than 3%) of BSA was observed during the experiments in Figure 5d. Moreover, flow speed should affect to penetration speed of analyte. Although the flow speed of the BSA solution was not controlled in this experiment (simple addition), employment of rotary pump will allow successful reproduction of more similar microenvironment to a blood capillary. These important optimizations of microenvironmental condition in the multilayered blood capillary analogs are now in progress.

3. Conclusions

In this report, we demonstrated for the first time a method to fabricate blood capillary analogs in biodegradable hydrogels possessing bilayered structures consisting of endothelial cells and smooth muscles cells to develop a 3D-bioassay system for blood capillaries. The multilayered architecture of blood capillaries was successfully reconstructed by our hierarchical cell manipulation technique, and tubular channels over 1 cm

in length were prepared inside biocompatible hydrogels. The demonstration of the barrier effect of the bilayer structures using BSA clarified the applicability of this bioassay system for in vitro blood capillary functions. Penetration experiments on drugs, drug carriers, and cancer cells using this blood capillary hydrogel system will be a powerful method to provide important and detailed knowledge which cannot be obtained by current in vivo bioassays. The transcytosis and endocytosis of serum albumin or peroxidases[26,27] into blood capillaries and the in vitro evaluation of the drug or gene deliveries through caveolae-mediated transcytosis into specific tissues[28] will be also possible using this technology, because the capillary species, such as an artery or vein, and the thickness of the SMC layer can be easily controlled. Furthermore, since these artificial blood capillaries were easily and safely collected from the surrounding γ-PGA-SS gels by the decomposition of the hydrogels with cysteine, and the obtained capillary has good blood compatibility (Figure S7, Supporting Information), this methodology is also useful for the tissue engineering and regenerative medicine fields.

4. Experimental Section

Preparation of γ-PGA-SS Hydrogels with Uniaxial Tubular Microchannels: Poly(γ-glutamic acid) (γ-PGA; M_w = 320 000; Meiji Seika), 1-ethyl-3-(3-dimethylaminopropyl)carbodiimide (EDC; Wako), and 2,2′-dithiobisethanamine dihydrochloride (cystamine; Tokyo Chemical Industry) were used without further purification. Fused silica capillaries of 150, 350, and 660 μm outer diameter (GL Science) were pretreated at 600 °C for 3 h in an electric furnace to remove the polyimide films coated on the surface. Next, after treating with 1 M sodium hydroxide at room temperature for 1 h, they were extensively washed with ultrapure water, and finally dried under vacuum. The outer diameters of the obtained capillaries were 120, 320, and 620 μm, respectively. Unless otherwise noted, silica capillaries of 620 μm diameter were used in this study. γ-PGA (2.0 unit mmol, 258 mg) was dissolved in 3.6 mL of 0.5 M $NaHCO_3$ aq., and EDC (2.0 mmol, 384 mg) was added into the solution. The reaction solution was stirred at 4 °C for 15 min, and then cystamine (0.75 mmol, 169 mg) dissolved in 400 μL of 1 mM GRGDS (Peptide Institute)/0.5 M $NaHCO_3$ aq. was added under magnetic stirring. The resultant solution was poured between 2 glass plates with a 2-mm silicon spacer, and silica capillaries arranged every 4 mm. After 3 h, the silica was gently extracted, and the obtained γ-PGA-SS hydrogels were washed with ultrapure water for 2 days to remove any remaining compounds. Finally, the gels were cut into arbitrary sizes for use. The swelling ratio of the gels was 20 ± 5 (n = 10) according to the following equation: swelling ratio = $(W_s–W_d)/W_d$, where W_s and W_d indicate the weight of the swollen and dried hydrogels, respectively. The channel sizes formed in the gels was analyzed from phase contrast microscopic images (n = 3), and are summarized in Figure 2c. For the preparation of γ-PGA-SS hydrogels with orthogonal-tubular channels, a gelling mould shown in Figure S2a (Supporting Information) was designed. A set of silica capillaries with 8 mm spacing were orthogonally laminated to form a 4-layered structure. The 3rd and 4th layers were arranged with a 4 mm parallel shift as compared to the 1st and 2nd layers, respectively. This silica set was incorporated into glass plates with a 5-mm silicon spacer, and the target hydrogels were prepared in the same manner as described above.

Fabrication of Cellular Multilayers in Tubular Channels: γ-PGA-SS gels (channel length: 1 cm) were washed with a 7/3 (v/v) ethanol/water solution, and immersed in phosphate-buffered saline (PBS) overnight. The gels were taken out from the solution, and the small amount of PBS remaining in the channels was removed, followed by washing with 50 mM Tris-buffer (pH = 7.4). In the same manner, a 50 mM Tris-HCl buffer solution (pH 7.4) of FN (0.2 mg/mL; Sigma) and a 50 mM Tris-HCl buffer solution of G (0.2 mg/mL; Wako) were alternatively injected in the channels in order to prepare FN-G nanofilms. Each step took 1 min at room temperature, and the Tris-HCl solution was used for washing at every step. After 9 steps ($(FN/G)_4FN$) of LbL assembly, the cell suspension was added into the channels and incubated for 48 h at 10 rpm. The cell concentrations were 5×10^6 cells/mL for the HUVECs (CAMBREX; passages 6 to 8), 4×10^6 cells/mL for the UASMCs (CAMBREX; passages 7–10), and 5×10^6 cells/mL for the hFCs (Sanko). The cells were cultured in smooth-muscle basal medium (SmBM; CAMBREX) containing human epidermal growth factor (hEGF), human fibroblast factor basic (hFGF-B), GA-1000, FBS and insulin, in endothelial basal medium-2 (EBM-2; CAMBREX, USA) containing hFGF-B, vascular endothelial growth factor (VEGF), R3-IGF-1 (IGF-1 = insulin-like growth factor 1), ascorbic acid, FBS, hEGF, and GA-1000, or in fibroblast basal medium (FBM; CAMBREX) containing insulin, hFGF-B, GA-1000, and FBS, respectively. The co-culture of the UASMCs and HUVECs was performed in a 1/1 (v/v) mixed solution of both media. For the lamination of the HUVECs onto the UASMCs, FN-G films were prepared onto the UASMC monolayer in the same manner as previously described, and the HUVEC suspension was injected and incubated for 48 h at 10 rpm.

Fluorescent Observations: UASMCs and HUVECs were labeled using cell tracker green (Molecular probe) and PKH26 red fluorescent cell linker kit (Sigma). For the immunostaining of the HUVECs, the samples were fixed in 10% formalin. After treatment with 1% bovine serum albumin (BSA)-PBS, the samples were incubated with a monoclonal mouse anti-human CD31 antibody (DakoCytomation) for 60 minutes at room temperature, and an Alexa Fluor 546-labeled goat anti-mouse IgG antibody (Molecular probe) to visualize the immunostaining. Fluorescent microscopy was performed with the Olympus disk scan system DSU-IX80-SET.

Decomposition of γ-PGA-SS Gels to Collect Bilayered Blood Vessel Tubes: Vascularized hydrogels with bilayered blood vessels composed of UASMCs and HUVECs were transferred into media containing 10 mM L-cysteine for 12 h. The obtained engineered tissues were then washed with PBS and observed by microscopy.

Permeability Experiments of BSA through Blood Capillaries in γ-PGA-SS Gels: A 0.45 mg/mL solution of tetramethylrhodamine-conjugated BSA (Rh-BSA; Sigma) dissolved in Dulbecco's modified eagle medium (DMEM) containing 10% fetal bovine serum (FBS) was injected into the channels. Confocal fluorescent images were taken every 15 min up to 60 min (same as Figure S6, Supporting Information), and the fluorescence intensity of the line-scanning (same as Figures 4f and Figure S4c, Supporting Information) over 400 μm, from positions –100 to 300 μm, was obtained and normalized against that at the –100 μm position using MetaMorph software (average of 10 values). The relative fluorescence intensity as compared to the initial intensity (0 min) was then calculated. From the temporal changes of the fluorescence intensity at the 300 μm position, the diffusion constant *k* was estimated.

Supporting Information

Supporting Information is available from the Wiley Online Library or from the author.

Acknowledgements

This work was supported mainly by PRESTO-JST, partly by Grant-in-Aid for JSPS fellows (20-703), an Industrial Technology Research Grant Program in 2006 (06B44017a) from NEDO of Japan, Grant-in-Aid for Scientific Research on Innovative Areas (21106514) from MEXT of Japan, NEXT Program from JSPS (LR026) and the Noguchi Institute.

Received: July 10, 2012
Revised: September 13, 2012
Published online: November 2, 2012

[1] B. C. Isenberg, J. Y. Wong, *Mater. Today* **2006**, *9*, 54.
[2] M. Hellstoröm, M. Kalén, P. Lindahl, A. Abramsson, C. Betsholtz, *Development* **1999**, *126*, 3047.
[3] A. C. Williams, B. W. Barry, *Adv. Drug Delivery Rev.* **2004**, *56*, 603.
[4] R. Gref, Y. Minamitake, M. T. Peracchia, V. Trubetskoy, V. Torchilin, R. Langer, *Science* **1994**, *263*, 1600.
[5] X. Michalet, F. F. Pinaud, L. A. Bentolila, J. M. Tsay, S. Doose, J. J. Li, G. Sundaresan, A. M. Wu, S. S. Gambhir, S. Weiss, *Science* **2005**, *307*, 538.
[6] J. C. Davila, R. J. Rodriguez, R. B. Melchert, D. Acosta, *Annu. Rev. Pharmacol. Toxicol.* **1998**, *38*, 63.
[7] N. J. Abbott, *Cell. Mol. Neurobiol.* **2000**, *20*, 131.
[8] Y. Matsumura, H. Maeda, *Cancer Res.* **1986**, *46*, 6387.
[9] M. R. Kano, Y. Bae, C. Iwata, Y. Morishita, M. Yashiro, M. Oka, T. Fujii, A. Komuro, K. Kiyono, M. Kaminishi, K. Hirakawa, Y. Ouchi, N. Nishiyama, K. Kataoka, K. Miyazono, *Proc. Natl. Acad. Sci. USA* **2007**, *104*, 3460.
[10] D. F. Baban, L. W. Seymour, *Adv. Drug Delivery Rev.* **1998**, *34*, 109.
[11] K. Y. Lee, D. J. Mooney, *Chem. Rev.* **2001**, *101*, 1869.
[12] A. S. Hoffman, *Adv. Drug Delivery Rev.* **2002**, *43*, 3.
[13] K. M. Chrobak, D. R. Potter, J. Tien, *Microvasc. Res.* **2006**, *71*, 185.
[14] K. Sato, K. Mawatari, T. Kitamori, *Lab Chip* **2008**, *8*, 1992.
[15] Y. Zheng, J. Chen, M. Craven, N. W. Choi, S. Totorica, A. Diaz-Santana, P. Kermani, B. Hempstead, C. Fischbach-Teschl, J. A. López, A. D. Stroock, *Proc. Natl. Acad. Sci. USA* **2012**, DOI:10.1073/pnas.1201240109.
[16] M. Matsusaki, T. Serizawa, A. Kishida, M. Akashi, *J. Biomed. Mater. Res.* **2005**, *73A*, 485.
[17] M. Matsusaki, M. Akashi, *Biomacromolecules* **2005**, *6*, 3351.
[18] M. Matsusaki, H. Yoshida, M. Akashi, *Biomaterials* **2007**, *28*, 2729.
[19] H. Yoshida, M. Matsusaki, M. Akashi, *Adv. Funct. Mater.* **2009**, *19*, 1001.
[20] H. Yoshida, M. Matsusaki, M. Akashi, *J. Biomater. Sci., Polym. Ed.* **2010**, *21*, 415.
[21] M. Matsusaki, K. Kadowaki, Y. Nakahara, M. Akashi, *Angew. Chem. Int. Ed.* **2007**, *46*, 4689.
[22] M. Matsusaki, *Bull. Chem. Soc. Jpn.* **2012**, *85*, 401.
[23] M. D. Pierschbacher, *Nature* **1984**, *309*, 30.
[24] G. Decher, J.-D. Hong, *Makromol. Chem., Macromol. Symp.* **1991**, *46*, 321.
[25] G. Decher, *Science* **1997**, *277*, 1232.
[26] L. Ghitescu, A. Fixman, M. Simonescu, N. Simonescu, *J. Cell Biol.* **1986**, *102*, 1304.
[27] C. Tiruppathi, T. Naqvi, Y. Wu, S. M. Vogel, R. D. Minshall, A. B. Malik, *Proc. Natl. Acad. Sci. USA* **2004**, *101*, 7699.
[28] D. P. Maclntosh, X. Y. Tan, P. Oh, J. E. Schnitzer, *Proc. Natl. Acad. Sci. USA* **2002**, *99*, 1996.